Published in final edited form as:
Nat Med. 2016 October ; 22(10): 1090–1093. doi:10.1038/nm.4161.

Characterization of progressive HIV-associated tuberculosis using 2-deoxy-2-[^{18}F]fluoro-D-glucose positron emission and computed tomography

H Esmail[1,2,3], **RP Lai**[4], **M Lesosky**[2,5], **KA Wilkinson**[2,4], **CM Graham**[4], **AK Coussens**[2], **T Oni**[2], **JM Warwick**[6], **Q Said-Hartley**[7], **CF Koegelenberg**[8], **G Walzl**[8,9], **JL Flynn**[10], **DB Young**[4,1], **CE Barry 3rd**[11,2,12,9], **A O'Garra**[4,13], and **RJ Wilkinson**[1,2,4]

[1]Department of Medicine, Imperial College London, United Kingdom

[2]Clinical Infectious Disease Research Initiative, Institute of Infectious Disease and Molecular Medicine, University of Cape Town, South Africa

[3]Radcliffe Department of Medicine, University of Oxford, United Kingdom

[4]The Francis Crick Institute Mill Hill Laboratory, London, United Kingdom

[5]Division of Epidemiology and Biostatistics, School of Public Health and Family Medicine, University of Cape Town, South Africa

[6]Department of Medical Imaging and Clinical Oncology, Stellenbosch University, Cape Town, South Africa

[7]Department of Radiology, Groote Schuur Hospital, Cape Town, South Africa

[8]Department of Medicine, Stellenbosch University, Cape Town, South Africa

[9]Department of Biomedical Sciences, Faculty of Medicine and Health Sciences, Stellenbosch University, Cape Town, South Africa

[10]Department of Microbiology and Molecular Genetics, University of Pittsburgh School of Medicine, United States of America

[11]Tuberculosis Research Section, National Institute of Allergy and Infectious Diseases, US National Institutes of Health, Bethesda, United States of America

[12]Department of Pathology, University of Cape Town, South Africa

Corresponding authors Dr. H. Esmail – hanif.esmail@ndcls.ox.ac.uk, Prof. R. J. Wilkinson – r.j.wilkinson@imperial.ac.uk.

Author Contributions

H.E., A.O'G., C.E.B. and R.J.W. designed the study with input from K.A.W., D.B.Y. and J.L.F.; H.E., T.O. and Q.S-H. screened participants for study entry; H.E., G.W. and C.F.K. collected samples and data and provided clinical care for participants during follow-up; J.M.W. led radiologists and nuclear medicine physicians reporting FDG-PET/CT scans; K.A.W. and H.E. processed samples; H.E., M.L., R.P.L analyzed data with advice and input from R.J.W., K.A.W., C.E.B., J.M.W., A.K.C., C.M.G., A.O'G. and J.L.F.; R.J.W. supervised data analysis; H.E. and R.J.W. wrote the manuscript, with early input from A.O'G., C.E.B., D.B.Y., M.L. and J.L.F. and subsequently all authors provided advice and approved the final manuscript.

Competing financial interests statements

The authors declare no competing financial interests

[13]National Heart and Lung Institute, Imperial College London, United Kingdom

Abstract

Tuberculosis is classically divided into states of latent infection and active disease. Using combined positron emission and computed tomography in 35 asymptomatic, antiretroviral therapy naïve, HIV-1 infected adults with latent tuberculosis, we identified ten individuals with pulmonary abnormalities suggestive of subclinical, active disease who were significantly more likely to progress to clinical disease. Our findings challenge the conventional two-state paradigm and may aid future identification of biomarkers predictive of progression.

Tuberculosis (TB) is classically divided into an active disease state (presence of symptoms characteristic of TB, in addition to microbiological confirmation of *Mycobacterium tuberculosis* (*M.tb*) or evidence of typical pathology identified radiographically or histologically) and a preceding non-infectious, latent infection state (evidence of immune sensitization by *M.tb* without evidence of active TB). Currently available tests for latent tuberculosis poorly predict who will develop disease[1]. We and others have suggested that this two state paradigm is an oversimplification, and that tuberculosis is characterised as a spectrum of infection states with transition from latent infection to active disease involving a subclinical phase of disease, during which pathology evolves prior to symptomatic presentation[2]. This view is supported by historical autopsy studies during which persons dying of causes other than TB frequently had evidence of minimally active disease[3, 4] and also by mass screening and prevalence surveys where asymptomatic persons are identified by either chest radiograph (CXR) abnormalities consistent with TB or sputum culture positive for *M.tb*[5, 6].

Chest radiography can be used to screen for evidence of subclinical TB, but is insensitive and prone to reader variability[7]. Sputum culture positivity in persons with a normal CXR is frequently described[8]; in these cases it is likely that CXR is insufficiently sensitive to detect the pulmonary pathology present. [^{18}F]-fluoro-2-deoxy-D-glucose (FDG) positron emission tomography combined with computed tomography (PET/CT) is a more sensitive imaging modality, which has the potential to detect early pathology in asymptomatic persons who are sputum culture negative. FDG uptake is increased in metabolically active cells; in TB this primarily relates to activated macrophages and neutrophils[9]. FDG-PET/CT has been used in the clinical investigation of TB and to describe evolving pathology in animal models of active and latent TB[10]. Here we used FDG-PET/CT to identify pathology consistent with subclinical pulmonary TB in asymptomatic HIV-1 infected persons, living in Khayelitsha, a township in Cape Town, South Africa, diagnosed with latent tuberculosis by a positive QuantiFERON Gold in tube (QFN-GIT) test and thus eligible for isoniazid preventive therapy (IPT).

We screened 265 HIV-1 infected, antiretroviral therapy (ART) naïve, adult outpatients with no history of previous TB (Supplementary Fig. 1). Notably ten (4%) of those screened were excluded for having positive sputum culture for *M.tb*, of whom five had no TB symptoms or chest radiographic (CXR) evidence of active TB (Supplementary Fig. 2). Thirty-five participants with a positive QFN-GIT but no history of IPT, a CXR without evidence of

Europe PMC Funders Author Manuscripts

active TB, CD4 T cell count ≥ 350/mm^3 who had no TB symptoms were recruited and underwent FDG-PET/CT following confirmation of negative sputum culture. Median CD4 count was 517/mm^3 (IQR 393 – 658) and 91% of participants were female. IPT was commenced following the initial PET/CT scan with close clinical follow-up. CD4 T cell threshold for ART initiation was below 350/mm^3.

Participants were TB symptom-free on the day of initial PET/CT scan with normal clinical parameters (Supplementary Table 1). Twenty-five participants (71.4%) had CT abnormalities within the lung parenchyma. These abnormalities were categorized into four groups; infiltrates, fibrotic scars, active nodules and discrete nodules (Figs. 1 and 2). The six participants with fibrotic scarring were significantly more likely to have infiltrates than those without scars, 50% (3/6) vs. 10% (3/29) ($P = 0.049$). There were significant differences in the anatomical distribution of abnormalities. Seventeen of the 18 (94%) infiltrates and scars were within the upper lobes (mainly apico-posteriorly located) (Figs 1a and 1b), in contrast to 33% of discrete nodules and 42% of active nodules ($P < 0.0001$) (Fig. 2e). However, compared to active nodules, discrete nodules were significantly more likely to be sub-pleurally located ($P = 0.001$) (Fig. 2c). We interpreted these abnormalities in relation to historical autopsy studies, particularly in regard to their spatial distribution and anatomical characteristics [3, 4, 11]. We determined the ten participants with either infiltrates and/or fibrotic scars, consistent with bronchogenic reactivation of TB ($n = 9$), or active nodules consistent with haematogenous spread of TB ($n = 1$) to have evidence of subclinical disease and the 25 participants with either normal lung parenchyma ($n = 10$) or discrete nodules only (anatomically consistent with Ghon foci of primary infection) ($n = 15$) to have no evidence of subclinical pathology.

Those with evidence of subclinical disease were significantly more likely to develop symptomatic active TB during six month follow-up; four out of ten participants required treatment with standard TB therapy (isoniazid, rifampicin for six months supplemented by pyrazinamide and ethambutol for the first two months (2HRZE/4HR)), compared to none of the 25 without evidence of subclinical pathology ($P = 0.0003$) (Fig. 1d). Of these four, two were confirmed by sputum culture (one with early evidence of cavitation) and two had progressive imaging changes consistent with active TB (Supplementary Fig. 3). All four developed TB symptoms a median of 32 days after PET/CT scan (range 7 – 90 days). Participants with subclinical pathology were also significantly more likely to have abnormal FDG uptake within mediastinal lymph nodes (80% vs. 32%, $P = 0.022$), but not within cervical or axillary lymph nodes ($P = 0.68$ and $P = 1.0$ respectively). Furthermore, in the 27 participants who underwent repeat FDG-PET/CT at six months after IPT or standard TB treatment, all of those with subclinical TB (six participants) had improvement in the baseline abnormalities within lung parenchyma or mediastinal lymph nodes compared to only one of the 21 participants with no evidence of subclinical TB ($P = 0.005$) (Fig. 1e, f). In all, 17 participants (48.6%) had evidence of mineralization within discreet nodules or lymph nodes, which was no different in those with or without evidence of subclinical pathology (50% vs 48%, $P = 0.91$). There were no significant differences in clinical characteristics between those with and without evidence of subclinical TB (Supplementary Table 1).

We have provided evidence of biological heterogeneity within what is currently diagnosed and managed as latent tuberculosis. Utilising FDG-PET/CT, as a research tool, we defined a subgroup of asymptomatic, HIV-1 infected persons, eligible for IPT, that had evidence of subclinical disease and who were at higher risk of disease progression. We were not able to fully elucidate the natural history of subclinical disease as all participants were treated with IPT or 2HRZE/4HR. This proof-of-concept study has implications for the optimal management of HIV-1 infected persons with evidence of immune sensitization by *M.tb*. Our findings may also facilitate future development of more practical biomarkers predicting disease progression.

Although FDG-PET/CT is a non-specific imaging tool, it is highly likely that the abnormalities we found related to subclinical TB and not alternative pathology. All participants classified as having subclinical TB who had a repeat scan showed evidence of improvement in baseline abnormalities in the regions of interest following specific therapy. Strict exclusion criteria and frequent clinical assessments minimised the possibility of alternative pathologies and in our study setting, TB is considerably more common as a cause of asymptomatic, upper lobe infiltration and scarring than alternative conditions (e.g. sarcoidosis or histoplasmosis)[12, 13].

Fibrotic scarring following spontaneous healing of TB infiltration is well established. Latently infected persons with evidence of fibrotic scarring are up to 15 times more likely to develop disease[14]. We show here that those with fibrotic scarring on FDG-PET/CT are significantly more likely to have infiltrates, however infiltrates did not arise directly from scars as previously thought [15] and could be located in distinct bronchopulmonary segments. These findings require confirmation but suggest that those with fibrotic scarring may represent a group at greater risk because of repeated episodes of subclinical reactivation. Participants with subclinical TB were significantly more likely to have FDG uptake within mediastinal lymph nodes, in keeping with a recently published case series of HIV-uninfected TB contacts[16].

Our findings support autopsy findings that TB pneumonia with bronchogenic spread is one of the earliest manifestations of pulmonary TB [17]. As disease progresses this may result in intermittent shedding of *M.tb* into sputum and pathology may eventually become visible on CXR. Dowdy *et al* modeling data from community prevalence surveys for undiagnosed culture positive TB have suggested that *M.tb* may be shed into sputum for up to 13.5 months prior to clinical presentation[18]. As pathology progresses, release of pro-inflammatory cytokines likely contribute to development of symptoms[19]. Active case finding by symptom screening or CXR typically shortens durations of symptoms at presentation. However the impact on transmission of these strategies has been disappointing and identification of subclinical disease at an earlier stage may be required to make an impact[20].

Zak and colleagues have recently described a 16-transcript signature in whole blood that identifies people within 12 months of clinically presenting with TB with 54% sensitivity and 83% specificity. Our work suggests that such biomarkers may identify infected individuals during the subclinical phase of disease [21].

Europe PMC Funders Author Manuscripts

Our findings raise issues around the optimal management of subclinical TB. As we have shown a proportion of HIV-1 infected adults with a negative screen for active (by sputum culture, CXR and symptom screen) and eligible for IPT have evidence of subclinical disease hence it is likely that isoniazid monotherapy is often inadvertently prescribed to persons with subclinical TB in clinical settings. Although this may be adequate for some, in a proportion this approach may not be successful in preventing clinical disease. Of note, Samandari *et al.* investigating six versus 36 months isoniazid in HIV-1 infected persons, showed rates of active TB increased shortly after cessation of therapy in the six-month group only in those with a positive tuberculin skin test. It is possible this reflects recrudescence of inadequately treated subclinical TB[22]. Multidrug therapy may be preferable, but whether six months of standard four-drug therapy is necessary to adequately treat subclinical TB is yet to be established. Traditionally studies to evaluate novel treatment regimens in those with asymptomatic TB infection have required large sample sizes and prolonged follow-up, our findings suggest that FDG-PET/CT could provide a potential surrogate endpoint to evaluate novel regimens for subclinical TB.

Online Methods

Recruitment of participants and controls

Ethical approval for this study was provided by the research ethics committees of the University of Cape Town (013/2011) and Stellenbosch University (N12/11/079). Recruitment and follow-up for the study took place between August 2011 and July 2013. All participants and controls were resident and recruited in Khayelitsha, a peri-urban township of Cape Town, South Africa where TB incidence is 917/100,000 and >95% of residents are of Xhosa ancestry. Informed consent was sought from all patient prior to screening and study entry.

The asymptomatic HIV-1 infected/ART naive persons with latent tuberculosis were recruited from local pre-ART wellness clinics. Participants were considered HIV-1 infected if they had a positive point of care (POC) test for HIV in their medical notes and, either a positive HIV-1 viral load and/or a positive HIV-1 ELISA. Potential participants were screened for active TB by symptom screen (cough > 1 week, haemoptysis, fever, night sweats, weight loss), digital posterior-anterior (PA) CXR, 2 x smear and culture (induced if necessary) and latent TB by QFN-GIT. Potential participants also underwent regular clinical assessment for symptoms and signs of TB over a six-week screening period. Potential participants were eligible for study participation if they met the following pre-established inclusion/exclusion criteria.

Inclusion criteria—HIV-1 infected, ART naïve, screening CD4 ≥ 350/mm^3, QFN-GIT positive at initial screening visit, age ≥ 18 years.

Exclusion criteria— Screening sputum culture positive for TB, symptoms or signs of active TB, evidence of active TB on initial screening CXR, evidence of any acute or unexplained chronic illness, previously diagnosed or treated TB, previous IPT, known recent contact of multi drug resistant (MDR)-TB, CXR abnormality known or suspected to relate to a condition other than TB, age > 50 years, smoker of > 30 pack years, occupational history

of mining or evidence of silicosis, previously diagnosed malignancy/ chronic lung infection/ chronic lung disease or chronic inflammatory condition, current corticosteroid use, uncontrolled diabetes mellitus, pregnant or planning pregnancy, breast feeding, inclusion in study to result in annual radiation exposure of > 50mSv, or any factor felt to significantly increase the participant's risk of suffering an adverse outcome.

Thirty-five eligible participants consented to study entry and underwent FDG-PET/CT, blood sampling and sputum culture. They were commenced on IPT (or standard TB therapy if microbiological or clinical evidence of active TB developed during follow-up) and had a repeat FDG-PET/CT after six months. No randomization took place.

Sample size considerations

For this study we took the novel approach of using of FDG-PET/CT as a research tool in human latent tuberculosis to define a subgroup with evidence of subclinical disease. There was no prior data to allow us to precisely establish the proportion of individuals that may have subclinical TB and hence the study was exploratory in this respect.

We determined that if less than approximately 20% of our participants had evidence of subclinical TB then our approach might need re-evaluation. We therefore pre-specified a planned initial evaluation after the first 18 participants had undergone baseline PET/CT imaging. We determined that if no participants had abnormalities consistent with subclinical TB at this stage then the true rate abnormalities would be unlikely to be greater than 20% (the upper bound of one-sided 97.5% binomial exact confidence interval would be 0.19) and planned to stop the study on grounds of futility. If at least one participant had abnormalities consistent with subclinical TB, we planned to continue to enrol a total of 35 participants. We determined that if no more than four of the 35 participants had evidence of subclinical TB, then the true rate of abnormalities in this population was unlikely to be greater than 27% (95% binomial exact confidence intervals are 0.03 and 0.27).

Chest radiograph reading

Chest radiographs were all performed using a digital X-Ray machine (Delft Oldeca DR or Phillips Essenta DR) and captured posterior-anteriorly with the participant standing in full inspiration. The Digital CXR images were viewed on 2 megapixel screens using the OsiriX version 3.8.1 32-bit (Pixemo, Bernex, Switzerland) software package and reported independently by 2 medically qualified researchers blinded to clinical details. CXR were reported using a structured reporting form to ensure CXR were fully assessed for evidence of TB and then classified as consistent with active TB, inactive TB, abnormal but not consistent with TB or normal according to modified CDC criteria [21]. We modified these criteria by retaining calcified granuloma as evidence of inactive TB as in previous versions of the guidance. Any disagreement in reporting was resolved by consensus, which if not achieved, was resolved by a 3rd reader.

Sputum processing for *Mycobacterium tuberculosis*

All sputum samples were processed in the accredited laboratories of the South African National Health Laboratory Services (NHLS) where auramine sputum smear and

mycobacteria growth indicator tube (MGIT) liquid TB culture were performed. Cultures were kept for 42 days before being classified as negative. For quality control (QC) sterile mock sputa were sent weekly to the laboratory. None of 209 mock sputa sent to the NHLS laboratory for TB culture between August 2011 and June 2014 were found to be positive for Mtb, demonstrating that cross contamination within this laboratory was very low. When the study began recruitment, sputum samples underwent auramine smear and MGIT culture, from 2012 MGIT culture was replaced by the GeneXpert MTB/RIF (Cepheid, Sunnyvale, CA) nucleic acid amplification test.

QuantiFERON Gold-in-tube

The QFN-GIT assay (Qiagen, Valencia, CA) was conducted and scored in accordance with manufacturer's instructions

FDG-PET/CT

FDG-PET/CT scans were performed at 2 different sites, both approximately 15 miles from the study site in Khayelitsha. Between August 2011 and May 2012 scans were performed at the Cape PET-CT centre in Panorama Mediclinic using a Siemens Biograph PET/CT machine. From June 2012 to July 2013, FDG-PET/CT scans were performed at the Western Cape Academic PET-CT centre at Tygerberg provincial hospital using a Phillips Gemini PET/CT machine. Imaging protocols were similar (PET – Injected dose of FDG = 4MBq/kg; CT Thorax – Kv = 120, mAs = 100, Collimation = 16x1.5, Field of View (FOV) = 600mm, Rotation time = 0.5 seconds, Matrix = 512, slice thickness = 3mm). All repeat imaging was performed on the same machine as the initial scan. The reporting of all images was carried out by the same group of radiologists and Nuclear Medicine physicians using the same structured report irrespective of where the scan took place.

Participants undergoing FDG-PET/CT fasted for six hours prior to the scan and were escorted to the PET/CT centre by a research worker. At the PET/CT centre a point of care assessment of blood glucose (BM) was performed to ensure BM < 11.1mmol/L. A POC pregnancy test was performed prior to scan on all female participants. Participants were prescribed 20mg propranolol orally to minimize brown fat uptake of FDG. Thirty minutes later 4MBq/kg of FDG was administered via a 22G cannula. Sixty minutes after FDG administration a PET/CT scan was performed. CT was limited to the thorax (neck to liver) to reduce radiation exposure. Total effective radiation dose per scan was approximately 10mSv (varying with body weight and height). A second PET/CT was performed after approximately six months using a similar dose of FDG and injection to scan time as the initial scan.

Images were reported using a structured report focusing on the lung parenchyma and mediastinal and hilar lymph nodes. Detailed reporting instructions were provided to all readers. The primary report of the PET/CT scan was provided by radiologists and Nuclear Medicine physicians at the Western Cape Academic PET/CT centre blinded to clinical details. Parenchymal lesions were categorized as infiltrates, fibrotic scars, active nodules or discrete nodules according to definitions below:

Europe PMC Funders Author Manuscripts

- **Infiltrate:** Irregular, poorly defined, airway consolidation which may have further evidence of radiographic activity (tree-in-bud appearance, cavitation) and may display increased FDG-PET activity (FDG uptake greater than background lung)
- **Fibrotic scar:** Linear fibrotic or fibro-cystic abnormalities slightly distorting the surrounding lung tissue with no radiographic signs of activity and may be calcified with only minimal FDG uptake.
- **Active nodule:** Small, spherical, non-calcified opacities within the lung parenchyma with poorly defined borders, which may have evidence of increased FDG-PET activity.
- **Discrete nodule:**Small, spherical opacities present within the lung parenchyma where the borders are clearly defined with no radiographic signs of activity and may be calcified with only minimal FDG uptake.

The size and location of lesions (both the lobar location and relationship to pleura and secondary lobule) were described. The lesions were also evaluated for radiographic signs of disease activity (e.g. cavitation, tree-in-bud appearance, poorly defined margin). FDG uptake within the parenchyma lesions was quantified by maximal standardized uptake value (SUV_{max}) and Visual Score (VS) (VS = 0 – No visible uptake of FDG, VS = 1 – FDG uptake within lesion greater that background lung parenchyma but less than mediastinal blood pool, VS = 2 – FDG uptake within lesion greater than mediastinal blood pool but less that liver, VS = 3 – FDG uptake within lesion greater than liver). Parenchymal lesions were considered to have abnormal FDG uptake if VS was ≥ 1. SUV_{max} and VS of mediastinal and hilar lymph nodes was assessed and FDG uptake was considered abnormal if VS ≥ 2. Mediastinal and hilar LN were also assessed for size (considered abnormal if short axis width was greater than 1 cm) and for evidence of mineralization. Abnormal lymph nodes were placed into one of the following lymph node basins following convention of the International Association for Study of Lung Cancer (IASLC); right or left superior mediastinal (IASLC 2 – 4), aortic (IASLC 5, 6), inferior mediastinal/subcarinal (IASLC 7 – 9), right or left hilar (IASLC 10 –14). In addition to the mediastinal and hilar lymph nodes, any abnormal uptake within cervical lymph nodes, axillary lymph nodes, upper abdominal lymph nodes and thymus were noted as well as any other pathological abnormalities between the mandible and base of liver. All PET/CT scans were reviewed by a second reader and any disagreement was resolved by a 3rd reader.

Categorization of participants

As described above, the primary reporting and final classification of parenchymal lesions (infiltrates, scars, nodules) found on FDG-PET/CT and assessment of their radiographic and metabolic activity was performed by nuclear medicine physicians and radiologists that were blinded to clinical details of participants, unaware of clinical outcome and not involved In laboratory components of study or data analysis.

The summary maps of different lesion types (infiltrates, scars, active nodules, discrete nodules) were created to identify patterns of spatial distribution for lesion types across the

participants. They were created to be anatomically accurate as follows. First an outline of each lesion of interest on CT was digitally propagated in the coronal plane and the location of the lesion then captured at the level of the carina using OsiriX software. The location of each lesion was then digitally traced onto a representative CXR, anchored by anatomical reference points. A similar approach used to create maps in the axial plane.

The radiographic abnormalities were then interpreted in relation to pathology described in historical autopsy studies identified through literature search, author collections and cross-referencing. We sought to identify studies published in English that were conducted in the pre-chemotheraputic era as a systematic evaluation pathology relating to tuberculous infection and early/minimal disease in persons predominantly dying of causes other than tuberculosis. Hence these were applicable to our imaging findings. Two studies were identified that provided description of different lesion types, their detailed anatomical location and had a clear methodology [3, 4] and were primarily used to interpret our radiographic findings along with a third study that focused solely on the anatomical distribution of primary lesions [11].

Infiltrates were determined to be consistent with reactivation and bronchogenic spread of TB with scarring representing spontaneous healing. Active nodules were determined to be consistent with haematogenous spread of TB. Participants with these three lesion types were considered to have evidence of subclinical disease. Discrete nodules were determined to be anatomically consistent with the Ghon foci of primary infection and participants in which these were the only parenchymal abnormality in addition to those with normal lung parenchyma were considered to have latent TB with no evidence of subclinical pathology.

Supplementary Material

Refer to Web version on PubMed Central for supplementary material.

Acknowledgments

This work was funded by the Wellcome Trust (090170, 104803), the Bill and Melinda Gates Foundation/Wellcome Trust Grand challenges in Global Health (37822), the intramural research program of NIH/NIAID and the National Institutes of Health (R01 HL106804). R.J.W. received support from the European Union (FP& HEALTH F3-2012-305578), National Research Foundation of South Africa (96841) and Research Councils of the UK via the Francis Crick Institute (10218 and U117565642) and Medical Research Council of South Africa (Strategic Health Innovations partnership).

References

[1]. Rangaka MX, Wilkinson KA, Glynn JR, Ling D, Menzies D, et al. Predictive value of interferon-gamma release assays for incident active tuberculosis: a systematic review and meta-analysis. Lancet Infect Dis. 2011; 12:45–55. [PubMed: 21846592]

[2]. Barry CE 3rd, Boshoff HI, Dartois V, Dick T, Ehrt S, et al. The spectrum of latent tuberculosis: rethinking the biology and intervention strategies. Nat Rev Microbiol. 2009; 7:845–855. [PubMed: 19855401]

[3]. Opie EL. The Focal Pulmonary Tuberculosis of Children and Adults. J Exp Med. 1917; 25:855–876. [PubMed: 19868127]

[4]. Medlar EM. The pathogenesis of minimal pulmonary tuberculosis; a study of 1,225 necropsies in cases of sudden and unexpected death. Am Rev Tuberc. 1948; 58:583–611. [PubMed: 18099839]

[5]. Golub JE, Mohan CI, Comstock GW, Chaisson RE. Active case finding of tuberculosis: historical perspective and future prospects. Int J Tuberc Lung Dis. 2005; 9:1183–1203. [PubMed: 16333924]

[6]. Corbett EL, MacPherson P. Tuberculosis screening in high human immunodeficiency virus prevalence settings: turning promise into reality. Int J Tuberc Lung Dis. 2013; 17:1125–1138. [PubMed: 23928165]

[7]. Koppaka, R.; Bock, N. How reliable is chest radiography?. Toman's tuberculosis case detection, treatment, and monitoring: questions and answers. Frieden, T., editor. Geneva: World Health Organization; 2004. p. 51-60.

[8]. Oni T, Burke R, Tsekela R, Bangani N, Seldon R, et al. High prevalence of subclinical tuberculosis in HIV-1-infected persons without advanced immunodeficiency: implications for TB screening. Thorax. 2011; 66:669–673. [PubMed: 21632522]

[9]. Mamede M, Higashi T, Kitaichi M, Ishizu K, Ishimori T, et al. [18F]FDG uptake and PCNA, Glut-1, and Hexokinase-II expressions in cancers and inflammatory lesions of the lung. Neoplasia. 2005; 7:369–379. [PubMed: 15967114]

[10]. Coleman MT, Maiello P, Tomko J, Frye LJ, Fillmore D, et al. Early Changes by (18)Fluorodeoxyglucose positron emission tomography coregistered with computed tomography predict outcome after *Mycobacterium tuberculosis* infection in cynomolgus macaques. Infect Immun. 2014; 82:2400–2404. [PubMed: 24664509]

[11]. Ghon, A. The Primary Lung Focus of Tuberculosis in Children. English Edition ed. New York: Paul B. Hoeber; 1916.

[12]. Rybicki BA, Iannuzzi MC. Epidemiology of sarcoidosis: recent advances and future prospects. Semin Respir Crit Care Med. 2007; 28:22–35. [PubMed: 17330190]

[13]. Craven SA, Benatar SR. Histoplasmosis in the Cape Province. A report of the second known outbreak. S Afr Med J. 1979; 55:89–92. [PubMed: 570729]

[14]. Steinbruck P, Dankova D, Edwards LB, Doster B, Livesay VT. Tuberculosis risk in persons with “fibrotic” x-ray lesions. Bull Int Union Tuberc. 1972; 47:135–159. [PubMed: 5077112]

[15]. Stead WW. Pathogenesis of the sporadic case of tuberculosis. N Engl J Med. 1967; 277:1008–1012. [PubMed: 6059578]

[16]. Ghesani N, Patrawalla A, Lardizabal A, Salgame P, Fennelly KP. Increased cellular activity in thoracic lymph nodes in early human latent tuberculosis infection. Am J Respir Crit Care Med. 2014; 189:748–750. [PubMed: 24628316]

[17]. Hunter RL. Pathology of post primary tuberculosis of the lung: An illustrated critical review. Tuberculosis. 2011; 91:497–509. [PubMed: 21733755]

[18]. Dowdy DW, Basu S, Andrews JR. Is passive diagnosis enough? The impact of subclinical disease on diagnostic strategies for tuberculosis. Am J Respir Crit Care Med. 2013; 187:543–551. [PubMed: 23262515]

[19]. Tramontana JM, Utaipat U, Molloy A, Akarasewi P, Burroughs M, et al. Thalidomide treatment reduces tumor necrosis factor alpha production and enhances weight gain in patients with pulmonary tuberculosis. Mol Med. 1995; 1:384–397. [PubMed: 8521296]

[20]. Kranzer K, Afnan-Holmes H, Tomlin K, Golub JE, Shapiro AE, et al. The benefits to communities and individuals of screening for active tuberculosis disease: a systematic review. Int J Tuberc Lung Dis. 2013; 17:432–446. [PubMed: 23485377]

[21]. Zak DE, Penn-Nicholson A, Scriba TJ, Thompson E, Suliman S, et al. A blood RNA signature for tuberculosis disease risk: a prospective cohort study. Lancet. 2016; 387:2312–2322. [PubMed: 27017310]

[22]. Samandari T, Agizew TB, Nyirenda S, Tedla Z, Sibanda T, et al. 6-month versus 36-month isoniazid preventive treatment for tuberculosis in adults with HIV infection in Botswana: a randomised, double-blind, placebo-controlled trial. Lancet. 2011; 377:1588–1598. [PubMed: 21492926]

[23]. U.S. Department of Health and Human Services. Tuberculosis Component of Technical Instructions for the Medical Examination of Aliens in the United States. 2008

Europe PMC Funders Author Manuscripts

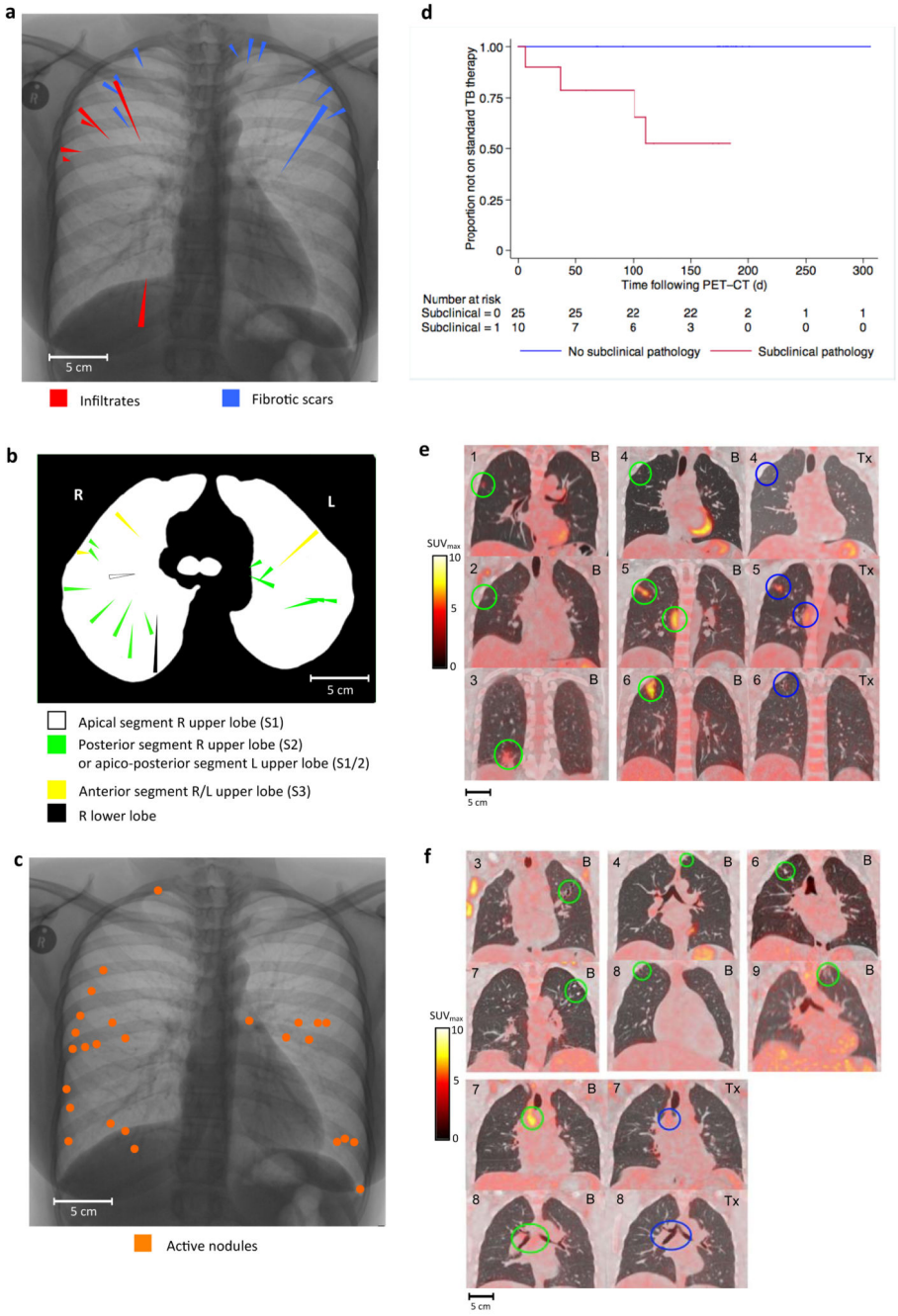

Figure 1. Radiological and clinical findings in participants with evidence of subclinical pathology (infiltrates, scars or active nodules)

a – Spatial overview of the FDG-PET/CT location of six infiltrates and 12 scars identified in nine participants in coronal plane. Lesions are represented on a single inverted CXR as triangles. Length of triangle is proportional to length of lesion.

b – Spatial overview of the FDG-PET/CT location of 18 infiltrates and scars in nine participants in the axial plane with broncho-pulmonary segment indicated.

Europe PMC Funders Author Manuscripts

c – Spatial overview of the FDG-PET/CT location of 26 active nodules found in one participant

d – Survival curve showing time to commencing standard 2HRZE/4HR for those with evidence of subclinical pathology ($n = 10$) and those without ($n = 25$), $P = 0.0003$ – log-rank test for equality)

e– Lesions from each of the six participants with infiltrates shown on fused FDG-PET/CT images in coronal plane. Participants uniquely numbered 1 – 6 in top left of image. Baseline scans denoted by “B” in top right corner with baseline lesions circled in green. Follow-up scans denoted by “Tx” in top right corner of image with lesions post-treatment circled in blue. For participants “4”, “5” and “6” the treatment received between scans was IPT, 2HRZE and 2HRZE/4HR respectively

f – Lesions from each of the six participants with scars (at least one example from each participant). Three participants numbered “3”, “4” and “6” also have infiltrates corresponding to Figure 1e. Lesions in baseline PET/CT scan circled in green. Mediastinal lymph nodes pre and post IPT circled green and blue respectively for participants “7” and “8”.

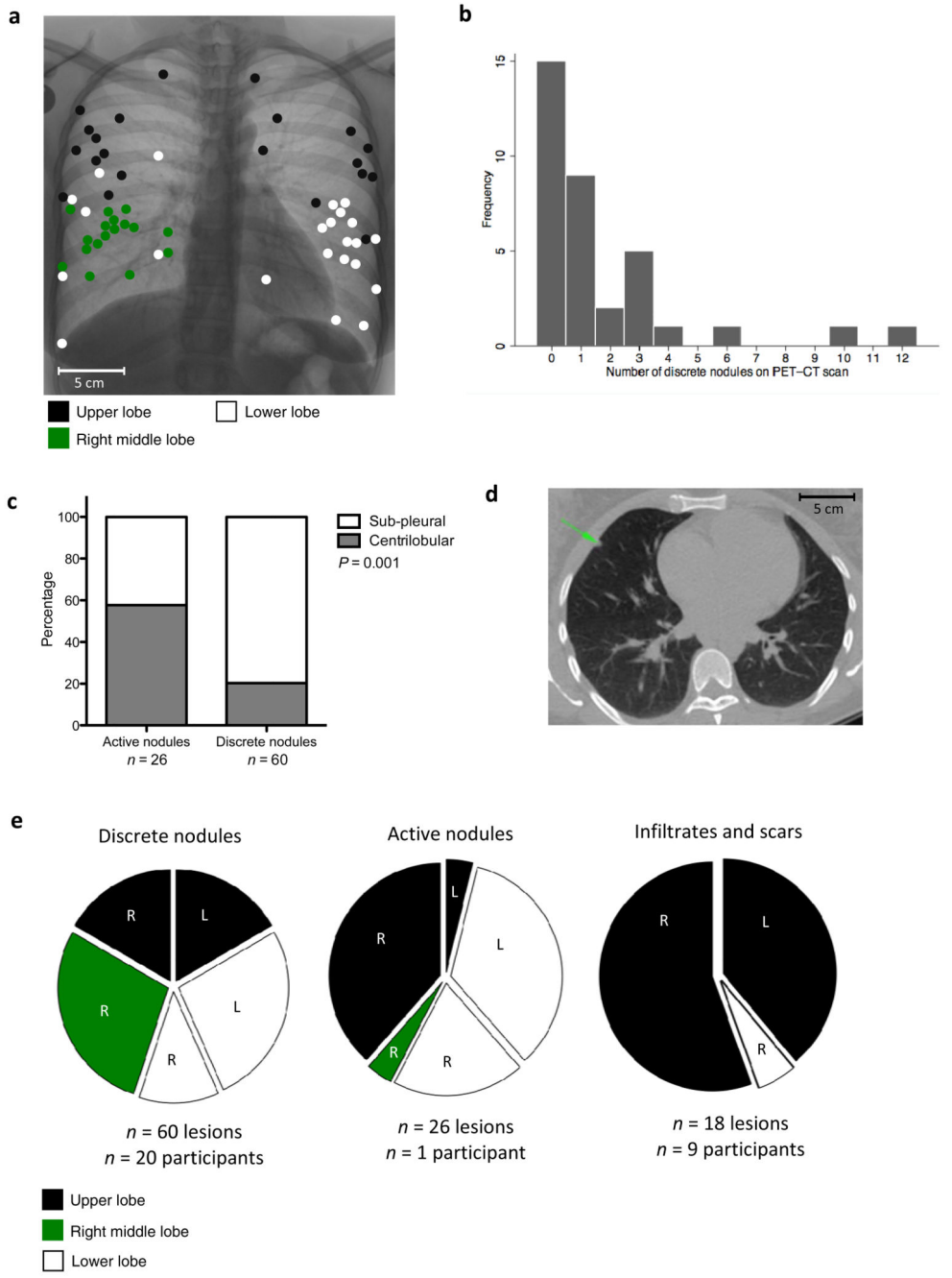

Figure 2. Radiological findings in participants with discrete nodules

a – Spatial overview of the FDG-PET/CT location of 60 discrete nodules in 20 participants (15 of which did not have other types of lesions) in the coronal plane. Lesions are represented as filled circles with colour denoting lobar location.

b – Frequency distribution showing number of discrete nodules found in lung parenchyma per participant.

Europe PMC Funders Author Manuscripts

c – Graph showing differences in lobular distribution of discrete compared to active nodules. Discrete nodules are significantly more likely to have a sub-pleural rather than centrilobular location, $P = 0.001$ - χ^2 test.

d – Example of a discrete nodule identified with green arrow on an axial section through CT scan.

e – Pie chart showing lobar distribution of discrete nodules, active nodules and infiltrates/ scars.

Europe PMC Funders Author Manuscripts